Fast Analysis of Scattering by Arbitrarily Shaped Three-Dimensional Objects Using the Precorrected-FFT Method

Xiaochun Nie and Le-Wei Li

***Abstract*--This paper presents an accurate and efficient method-of-moments solution of the electrical-field integral equation (EFIE) for large, three-dimensional, arbitrarily shaped objects. In this method, the generalized conjugate residual method (GCR) is used to solve the matrix equation iteratively and the precorrected-FFT technique is then employed to accelerate the matrix-vector multiplication in iterations. The precorrected-FFT method eliminates the need to generate and store the usual square impedance matrix, thus leading to a great reduction in memory requirement and execution time. It is at best an $O(N \log N)$ algorithm and can be modified to fit a wide variety of systems with different Green's functions without excessive effor[1]t. Numerical results are presented to demonstrate the accuracy and computational efficiency of the technique.**

***Indexs*--precorrected-FFT method, method-of-moments, electrical-field integral equation, electromagnetic scattering**

I. INTRODUCTION

Integral equation methods are widely used for the solution of electromagnetic scattering problems. In this approach, the problem is first formulated in terms of an appropriate integral equation and then reduced to system of linear equations using the method of Moments (MoM). If iterative methods are used to solve the linear system, the application of the coefficient matrix to sequence of vectors is required in the solution process. Each of these evaluations requires $O(N^2)$ operations, where N is the number of unknowns, making it prohibitively expensive for large problems.

In recent years, a number of techniques have been proposed to speed up the evaluation of matrix-vector multiplications, including the fast multipole method (FMM), the adaptive integral method (AIM), the conjugate gradient-fast Fourier transform method (CG-FFT), etc.. The fast multipole method (FMM) [1,2] and its extension, the multilevel fast multipole algorithm (MLFMA) [3] reduce the computation complexity to $O(N^{1.5})$ and $O(N \log N)$ respectively by performing the non-near-field interactions efficiently with the aid of the multipole expansion of the fields. **T**heir dependence on the Green's functions restricts their applications to some extent. The adaptive integral method (AIM) [4] achieves its central processing unit (CPU) and memory reduction by mapping the original moment method discretization onto a uniform grid and then applying the fast Fourier transform (FFT) to carry out the matrix-vector multiplication. This approach can be used to a wide variety of kernels and reduces the computational complexity and memory requirement to $O(N^{1.5})$ and $O(N^{1.5} \log N)$ respectively. The CG-FFT [5] is a powerful fast algorithm except that it requires the integral equation be discretized on uniform rectangular grids. Since modeling an arbitrary geometry with uniform rectangular grids necessitates a stair-case approximation which makes the final solution inaccurate, this is considered as the most serious drawback of the CG-FFT.

One approach which can overcome this drawback is the precorrected-FFT method. This technique was originally proposed by Philips and White [6,7] to solve electrostatic integral equation associated with capacitance extraction problems and extended to 2-dimensional scattering problems by the authors [8] recently. In this paper, the precorrected-FFT method is used to solve scattering from 3-dimensional arbitrary objects. Like the AIM, the precorrected-FFT method uses discretization based on Rao-Wilton-Glisson (RWG) [9] functions and then projecting the triangular subdomain basis functions onto a uniform grid. Then the long-range part of the field is represented by current

[1] Xiaochun Nie is with High Performance Computation for Engineered Systems (HPCES) Programme, Singapore-MIT Alliance (SMA), Singapore/USA 119260/02139 (telephone: 65-874-5154, e-mail: smaniexc@ nus.edu.sg).

Le-Wei Li is with High Performance Computation for Engineered Systems (HPCES) Programme, Singapore-MIT Alliance (SMA), Singapore/USA 119260/02139 and Department of Electrical and Computer Engineering, The National University of Singapore. (e-mail: lwli@nus.edu.sg).

Jacob K. White is with High Performance Computation for Engineered Systems (HPCES) Programme, Singapore-MIT Alliance (SMA), Singapore/USA 119260/02139 and Department of Electrical Engineering and Computer Science, Massachusetts Institute of Technology, United States. (e-mail: white@mit.edu).

distributions lying on this uniform grid, rather than by series expansions as in fast multipole algorithms. This grid representation allows the Fast Fourier Transform (FFT) to be used to efficiently perform the matrix-vector multiplication. The resulting algorithm has at best a memory requirement proportional to $O(N)$ and an operation count for the matrix-vector multiplication proportional to $O(N \log N)$. In comparative to the AIM, the projection operator of the precorrected-FFT is in a much simpler form and has higher accuracy. The precorrected-FFT method employs δ functions on the uniform grid and generates the projection operators between the uniform and irregular meshes via multipole expansions of the vector and scalar potentials while the AIM generates projections by equating a finite number of multipole moments of the basis functions, which is a quite complex procedure. And since the fields at any point can be fully determined by the vector and scalar potentials, the projections of the precorrected-FFT method have better accuracy than those of the AIM. Due to this, the precorrected-FFT can have much coarser grid and smaller near-field threshold distance than the AIM, thus resulting in much lower memory requirement and computational cost. Numerical results will be presented to demonstrate this advantage. It should be noted that the precorrected-FFT method can also be applied to any integral equation as long as the convolution property is retained.

II. PROBLEM FORMULATION

Because the electric field integral equation (EFIE) has the advantage of being applicable to both open and closed bodies, whereas the MEIE only to closed surfaces, we initiate our analysis from the EFIE. Consider an arbitrarily shaped 3-D conducting object illuminated by an incident plane wave $\boldsymbol{E}^i$. The EFIE is given by

$$\hat{n} \times [\, j\omega \boldsymbol{A}(\boldsymbol{r}) + \nabla \Phi(\boldsymbol{r})] = \hat{n} \times \boldsymbol{E}^i(\boldsymbol{r}) \tag{1}$$

where the magnetic vector potential $\boldsymbol{A}$ and electric scalar potential Φ are defined as follows, respectively,

$$\boldsymbol{A}(\boldsymbol{r}) = \frac{\mu}{4\pi} \int_S \boldsymbol{J}(\boldsymbol{r}') \frac{e^{-jk|\boldsymbol{r}-\boldsymbol{r}'|}}{|\boldsymbol{r}-\boldsymbol{r}'|} dS' \tag{2}$$

$$\Phi(\boldsymbol{r}) = -\frac{1}{4\pi j\omega\varepsilon} \int_S \nabla_s \cdot \boldsymbol{J}(\boldsymbol{r}') \frac{e^{-jk|\boldsymbol{r}-\boldsymbol{r}'|}}{|\boldsymbol{r}-\boldsymbol{r}'|} dS' \tag{3}$$

In the above equations, $\hat{n}$ is the unit normal vector of the surface S of the conducting object, and $\boldsymbol{J}$ is the unknown current on S. A harmonic time dependence $e^{j\omega t}$ is assumed and suppressed.

For numerical solution of the EFIE, the surface is discretized into small triangular patches, and the current $\boldsymbol{J}$ is expanded using the Rao-Wilton-Glisson (RWG) basis functions $\boldsymbol{f}_n(\boldsymbol{r})$ [9]

$$\boldsymbol{J}(\boldsymbol{r}) = \sum_{n=1}^{N} I_n \boldsymbol{f}_n(\boldsymbol{r}) \tag{4}$$

where N denotes the number of unknowns, and I_n stands for the unknown coefficients. Applying the method of moments results in a linear system

$$\boldsymbol{ZI} = \boldsymbol{V} \tag{5}$$

In Eqn. (5) the impedance matrix $\boldsymbol{Z}$ and the vector $\boldsymbol{V}$ have the elements given by, respectively,

$$\begin{aligned} \mathbf{Z}_{ij} = {} & \frac{j\omega\mu}{4\pi} \int_{T_i} \int_{T_j} \boldsymbol{t}_i(\mathbf{r}) \cdot \boldsymbol{f}_j(\mathbf{r}') G(\mathbf{r}, \mathbf{r}') d\mathbf{r}' d\mathbf{r} \\ & + \frac{1}{4\pi j\omega\varepsilon} \int_{T_i} \int_{T_j} \nabla \cdot \boldsymbol{t}_i(\mathbf{r}) \nabla' \cdot \boldsymbol{f}_j(\mathbf{r}') G(\mathbf{r}, \mathbf{r}') d\mathbf{r}' d\mathbf{r} \end{aligned} \tag{6}$$

$$V_i = \int_{T_i} \boldsymbol{t}_i(\boldsymbol{r}) \cdot \boldsymbol{E}^i(\boldsymbol{r}) d\boldsymbol{r} \tag{7}$$

where $\boldsymbol{t}_i$ and $\boldsymbol{f}_j$ represent the testing and basis functions, respectively, T_i and T_j denote their supports, and G is the scalar Green's function in free space. Since the impedance matrix $\boldsymbol{Z}$ is fully populated, demanding $O(N^2)$ storage, the solution of Eqn. (5) requires $O(N^3)$ operations in a direct scheme or $O(N^2)$ operations per iteration in an iterative scheme. This memory requirement and computational complexity will cause serious memory limitations and make the method computationally intractable when the geometrical dimension is electrically large. The difficulties can be overcome by utilizing the precorrected-FFT method. Since the efficiency of the method is also determined by the convergence of the iterative algorithm, the generalized conjugate gradient method [10] is used to solve the matrix equation for a faster convergence.

III. THE PRECORRECTED-FFT APPROACH

Like other fast algorithms, the precorrected-FFT method is also based on the idea of directly computing only those portions of $\boldsymbol{ZI}$ associated with the near-zone interactions and evaluating those with far-zone interactions in an approximate manner.

Application of the precorrected-FFT method requires that the whole geometry be enclosed in a uniform right-parallelepiped grid after it has been discretized into triangular elements. The elements are sorted into the cells formed by the grid, with each cell containing only a few elements. Figure 1 shows a discretized sphere, with the associated space subdivided into a $8 \times 8 \times 8$ grid. Based on the fact that fields at evaluation points distant from an

element can be accurately computed by representing the given element's current and charge distributions using a small number of weighted point currents and charges, the matrix–vector multiplication can be approximated in a four-step procedure as follows: (1) to project the element singularity distributions to point singularities on the uniform grid, (2) to compute the fields at the grid points due to the singularities at the grid points using the FFT, (3) to interpolate the grid point fields onto the elements, and (4) to directly compute nearby interactions. This process is summarized in Figure 2.

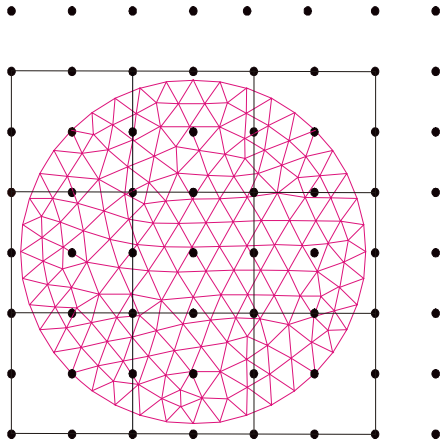

Figure 1. Side view of the P-FFT grid for a discretized sphere ($p = 3$)

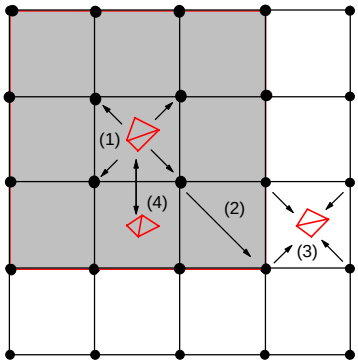

Figure 2. 2-D representation of the procedures of the precorrected-FFT algorithm **(** $p = 2$ **)**

3.1 Projecting the element singularity distributions to point singularities on the uniform grid

Firstly, we describe the construction of the projection operator W. Assume the mth RWG basis function defined on the mth edge is contained in a given cell k. So the point current and charge distributions on the grid surrounding the mth edge are used to represent the current and charge distributions of the two m th RWG patches. Point singularities on the grid can be set at the cell vertices (grid-order $p = 2$), or at half the spacing of the vertices (grid-order $p = 3$), etc, as desired for accuracy. N_c test points are selected on the surface of a sphere of radius r_c whose center is coincident with the center of the cell k. We first consider the projection of the current. Enforcing the magnetic vector potential due to the currents at the p^3 points on the grid to match that due to the original current distribution on the element at the test points, we obtain

$$\boldsymbol{A}_q^{pt} = \tilde{\boldsymbol{A}}_q^{gt}, \qquad q = 1,2,\cdots N_c \tag{8}$$

where $\boldsymbol{A}_q^{pt}$ denotes the vector potential at the qth test point due to the original patch current and $\tilde{\boldsymbol{A}}_q^{gt}$ represents that due to the grid currents. They can be computed by

$$\boldsymbol{A}_q^{pt}(\boldsymbol{r}_q^t) = \frac{\mu}{4\pi}\int_S I_m \boldsymbol{f}_m(\boldsymbol{r}')\frac{e^{-jk\left|\boldsymbol{r}_q^t-\boldsymbol{r}'\right|}}{\left|\boldsymbol{r}_q^t-\boldsymbol{r}'\right|}dS' \tag{9}$$

$$\tilde{\boldsymbol{A}}_q^{gt}(\boldsymbol{r}_q) = \frac{\mu}{4\pi}\int_S \sum_{n=1}^{p^3}\left(J_{x,n}\hat{\boldsymbol{x}} + J_{y,n}\hat{\boldsymbol{y}} + J_{z,n}\hat{\boldsymbol{z}}\right) \cdot \delta(\boldsymbol{r}_n - \boldsymbol{r}')\frac{e^{-jk\left|\boldsymbol{r}_q^t-\boldsymbol{r}'\right|}}{\left|\boldsymbol{r}_q^t-\boldsymbol{r}'\right|}dS' \tag{10}$$

where $\boldsymbol{r}_q^t$ and $\boldsymbol{r}_n$ are the position vectors at the qth test point and the nth grid point, respectively, $\delta(x)$ is the Dirac delta function, and $J_{x,n}$, $J_{y,n}$ and $J_{z,n}$ are the three components of the current at the nth grid point. Substituting (9) and (10) into (8) for all N_c test points and decomposing the patch currents into three components yield

$$\boldsymbol{P}_x^{gt}\hat{J}_x = \boldsymbol{P}_x^{pt} I_m \tag{11a}$$

$$\boldsymbol{P}_y^{gt}\hat{J}_y = \boldsymbol{P}_y^{pt} I_m \tag{11b}$$

$$\boldsymbol{P}_z^{gt}\hat{J}_z = \boldsymbol{P}_z^{pt} I_m \tag{11c}$$

where $(\hat{J}_x, \hat{J}_y, \hat{J}_z) \in R^{p^3\times 1}$ are the vectors consisting of the current components in the grid points,

$(\boldsymbol{P}_x^{gt}, \boldsymbol{P}_y^{gt}, \boldsymbol{P}_z^{gt}) \in R^{N_c \times p^3}$ are the mappings between grid currents and test point potentials, given by

$$\boldsymbol{P}_{x,y,z}^{gt}(q,n) = \frac{\mu}{4\pi} \frac{e^{-jk\left|\boldsymbol{r}_q^t - \boldsymbol{r}_n\right|}}{\left|\boldsymbol{r}_q^t - \boldsymbol{r}_n\right|} \tag{12}$$

By construction, the relative positions of the grid currents and the test points are identical for each cell, and therefore $\boldsymbol{P}_{x,y,z}^{gt}$ are the same for each cell. $\boldsymbol{P}_{x,y,z}^{pt} \in R^{N_c \times N(k)}$ are the mappings between patch currents and test point potentials, $N(k)$ is the number of the basis functions contained in cell k. $\boldsymbol{P}_x^{pt}$ is given by

$$\boldsymbol{P}_x^{pt}(q,m) = \frac{\mu}{4\pi} \int_S \boldsymbol{f}_m(\boldsymbol{r}') \cdot \hat{\boldsymbol{x}} \frac{e^{-jk\left|\boldsymbol{r}_q^t - \boldsymbol{r}'\right|}}{\left|\boldsymbol{r}_q^t - \boldsymbol{r}'\right|} dS' \tag{13}$$

while $\boldsymbol{P}_y^{pt}$ and $\boldsymbol{P}_z^{pt}$ have a form similar to $\boldsymbol{P}_x^{pt}$. Since the collocation in (11) is linear in the patch and grid current distributions, the contribution of the mth basis function in cell k to $\hat{J}_x, \hat{J}_y, \hat{J}_z$ can be represented by three column vectors $W_{x,y,z}(k,m)$ given by

$$W_{x,y,z}(k,m) = \left[\boldsymbol{P}_{x,y,z}^{gt}\right]^+ \boldsymbol{P}_{x,y,z}^{pt,m} \tag{14}$$

where $\boldsymbol{P}_{x,y,z}^{pt,j}$ denotes the mth column of $\boldsymbol{P}_{x,y,z}^{pt}$ and $\left[\boldsymbol{P}_{x,y,z}^{gt}\right]^+$ indicates the generalized inverse of $\boldsymbol{P}_{x,y,z}^{gt}$. Since the matrices $\boldsymbol{P}_{x,y,z}^{gt}$ are small and the same for each cell, the relative computational cost of computing $\left[\boldsymbol{P}_{x,y,z}^{gt}\right]^+$ is insignificant. By using the vectors $W_{x,y,z}(k,m)$, we can project the current basis function $\boldsymbol{f}_m$ onto the p^3 grid points surrounding cell k.

For any patch current $I_m \boldsymbol{f}_m$ ($m = 1,2,\cdots N(k)$) in cell k, this projection operation generates a subset of the grid currents $\hat{J}_x, \hat{J}_y, \hat{J}_z$. The contribution to $\hat{J}_x, \hat{J}_y, \hat{J}_z$ from the currents in cell k is generated by summing over all the currents in the cell. Note that patch currents outside cell k may contribute to some of the elements of $\hat{J}_x, \hat{J}_y, \hat{J}_z$ in the case of shared grid currents.

Similarly, by enforcing the electric scalar potential due to the p^3 grid charges to match that due to the actual patch charge distribution at the test points, we can construct the charge projection operator

$$W_c(k,m) = \left[\boldsymbol{P}_c^{gt}\right]^+ \boldsymbol{P}_c^{pt,m} \tag{15}$$

where

$$\boldsymbol{P}_c^{gt}(q,n) = \frac{1}{4\pi\varepsilon} \frac{e^{-jk\left|\boldsymbol{r}_q^t - \boldsymbol{r}_n\right|}}{\left|\boldsymbol{r}_q^t - \boldsymbol{r}_n\right|} \tag{16}$$

$$\boldsymbol{P}_c^{pt}(q,m) = \frac{-1}{4\pi j\omega\varepsilon} \int_S \nabla \cdot \boldsymbol{f}_m(\boldsymbol{r}') \frac{e^{-jk\left|\boldsymbol{r}_q^t - \boldsymbol{r}'\right|}}{\left|\boldsymbol{r}_q^t - \boldsymbol{r}'\right|} dS' \tag{17}$$

It should be noted that the mapping $\boldsymbol{P}_c^{gt}$ is similar to $\boldsymbol{P}_x^{gt}$ except for a constant, so the general inverse of $\boldsymbol{P}_c^{gt}$, $\left[\boldsymbol{P}_c^{gt}\right]^+$ can be readily obtained from $\left[\boldsymbol{P}_x^{gt}\right]^+$.

The accuracy of the above projection scheme depends on the proper selection of the test points $\boldsymbol{r}^t$. For high accuracy, the test points should be chosen to be abscissas of a high-order quadrature rule. It can be shown that the error in potentials due to the grid-singularity approximations of the singularity distributions contained within a sphere of radius a, at a distance r from the center of the distribution, is of order $(a/r)^{(M+1)/2}$ if the test points are chosen to be the nodes of a quadrature rule accurate to order M [6,7].

3.2 Computing grid fields due to grid singularities using FFT

Once the patch currents and charges have been projected to uniform grids, the vector potentials at the grid points due to the grid currents can be computed by the following 3-dimensional convolutions

$$\begin{aligned} \hat{A}_{x,y,z}(i,j,k) &= H\hat{J}_{x,y,z} \\ &= \sum_{i',j',k'} h(i-i', j-j', k-k') \\ &\quad \cdot \hat{J}_{x,y,z}(i',j',k') \end{aligned} \tag{18}$$

where (i,j,k) and (i',j',k') are triplets specifying the grid points and $h(i,j,k)$ is given by

$$h(i,j,k) = \frac{\mu}{4\pi} \frac{e^{-jk\sqrt{(i\Delta x)^2 + (j\Delta y)^2 + (k\Delta z)^2}}}{\sqrt{(i\Delta x)^2 + (j\Delta y)^2 + (k\Delta z)^2}} \tag{19}$$

with $(\Delta x, \Delta y, \Delta z)$ being the edge lengths of the grid. $h(0,0,0)$ can be arbitrarily defined, but is usually set to zero for simplicity. The convolutions in Eqn. (18) can be rapidly computed by using the Fast Fourier Transform (FFT) [11] ,

$$\hat{A}_{x,y,z} = F^{-1}\left(\tilde{H} \cdot \tilde{J}_{x,y,z}\right) \quad (20)$$

where F^{-1} denotes the inverse FFT, while $\tilde{H}$ and $\tilde{J}$ are the FFT forms of $h(i,j,k)$ and $\hat{J}(i,j,k)$, respectively. The scalar potentials at the grid points due to the grid charges can be computed in the same way,

$$\hat{\Phi}(i,j,k) = H\hat{q} = \sum_{i',j',k'} h_q(i-i', j-j', k-k') \hat{q}(i',j',k') \quad (21)$$

with

$$h_q(i,j,k) = \frac{1}{4\pi\varepsilon} \frac{e^{-jk\sqrt{(i\Delta x)^2+(j\Delta y)^2+(k\Delta z)^2}}}{\sqrt{(i\Delta x)^2+(j\Delta y)^2+(k\Delta z)^2}} \quad (22)$$

In practice, each convolution requires one forward and one inverse 3-D FFT. The discrete Fourier transform of the kernel matrices, $\tilde{H}$, needs to be computed only once through out the algorithm because $h(i,j,k)$ and $h_q(i,j,k)$ are the same except for a constant and are only decided by the grid distribution.

3.3 Interpolating grid potentials onto elements

Once the grid potentials have been computed, they must be interpolated to the element in each cell. This process is essentially the same as the projecting process. It has been proved that the projection and interpolation operators have comparable accuracies [7].

Assume $[V(k,j)]^T$ denotes the operator which interpolates potentials at the grid points onto the patch coordinates. Thus, projection, followed by convolution and interpolation, gives the grid approximation A_G and Φ_G to the patch potentials which can be represented as

$$A_G = V^T HWJ \quad (23)$$

$$\Phi_G = V^T HW(\nabla \cdot J) \quad (24)$$

3.4 Computing near-zone interactions directly

Since the error due to the grid approximation is inversely proportional to the interaction distance, the interactions between nearby patches have been poorly approximated in the above three steps. To get accurate results, it is necessary to compute the near-zone interactions directly and remove the inaccurate contribution from the use of the grid. This process is referred to as "precorrection".

Define a "precorrected" direct interaction operator

$$\tilde{P}(k,l) = P(k,l) - V(k)^T H(k,l) W(l). \quad (25)$$

The exact vector potemtial $A(k)$ and scalar potential $\Phi(k)$ for each cell k can be obtained by

$$A(k) = A_G(k) + \sum_{l \in M(k)} \tilde{P}(k.l) J_l, \quad (26)$$

$$\Phi(k) = \Phi_G(k) + \sum_{l \in M(k)} \tilde{P}(k,l)(\nabla \cdot J_l) \quad (27)$$

where $A_G(k)$ and $\Phi_G(k)$ are the grid-approximations to $A(k)$ and $\Phi(k)$, respectively, including the inaccurate near-zone portions. $M(k)$ denotes the indices of the set of cells which are "close to" cell k. The second term each in (26) and (27) represents the near-zone interactions that can be computed directly. Because for each k, $M(k)$ is a small set and each matrix $\tilde{P}(k,l)$ is also small, the precorrection process is also a sparse operation.

Combining the above steps leads to the precorrected-FFT algorithm. The effect of this algorithm is so made as to replace the dense matrix-vector product $\boldsymbol{PJ}$ with the sparse operation $[\tilde{P} + V^T HW]J$.

VI. NUMERICAL RESULTS AND DISCUSSIONS

In this section, several numerical results are presented to demonstrate the accuracy and efficiency of the method described above. Fig. 3 shows the bistatic RCS computed by the precorrected-FFT method and the analytic solution (Mie-series) [15] for a sphere of $ka = 15$. The sphere is discretized into 14160 triangles and has 21240 unknowns. The dimension of the FFT is $26 \times 26 \times 26$. We choose $r_{thr} = 0.5\lambda$, so N_{near} is 12855328. The precorrected-FFT requires about 130 MB memory and takes 9 hours to compute the solution a Pentium 1G PC.

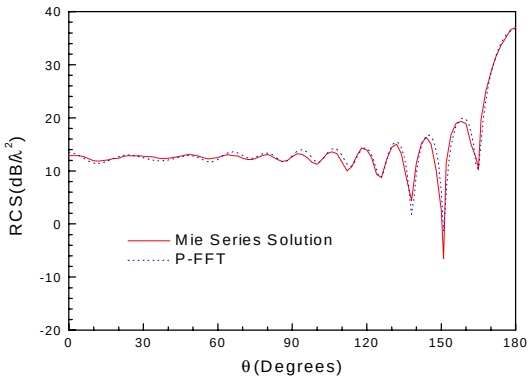

Figure 3. Bistatic RCS for a sphere of $ka = 15$ (θ polarization)

It is estimated that the conventional MoM requires approximately 3.36 GB of memory and will take about 80 hours for the same problem. It can be seen that, for this example, the precorrected-FFT yields a memory saving of about 97% and an over 88% reduction in the CPU time.

The last example shown in Fig. 4 is a benchmark cone-sphere with gap. The geometry parameters can be found in [16]. Fig. 5 and 6 give its monostatic RCS in two polarizations in the plane of $\theta = 90^o$ at 3 GHz. The object is discretized into 14100 unknowns and enclosed in a $48 \times 12 \times 12$ grid. To accelerate the convergence, we use the current solution from the previous angle with phase correction as the initial guess for the next angle. For a 0.5λ threshold distance, N_{near} is 17355998, about 8.73% that of N^2. The total memory requirement is about 9.93% that of the conventional MoM. The memory saving is not as dramatic as in last example because that the elements of this object distribute in a denser manner. The P-FFT takes 60 hours for 91 incident angles on a Pentium 1G PC while the MoM is estimated to require 900 hours by extrapolation. A reasonably good agreement is observed between the P-FFT solution and the measured results, demonstrating the P-FFT algorithm has a good accuracy. Fig.7 shows the number of iterations as a function of the incident angles required for a relative error of 0.8×10^{-3}. It can be seen that the appropriate initial guess reduces the number of iterations significantly.

Furthermore, we also found that, unlike some other fast algorithms such as FMM, both the convergence rate and condition of the P-FFT system remains unchanged from the original MoM system. This is of critical importance for fast iterative solutions because an increase in the iteration count would annul the faster computation of the matrix-vector product.

Figure 4. The benchmark cone-sphere with gap

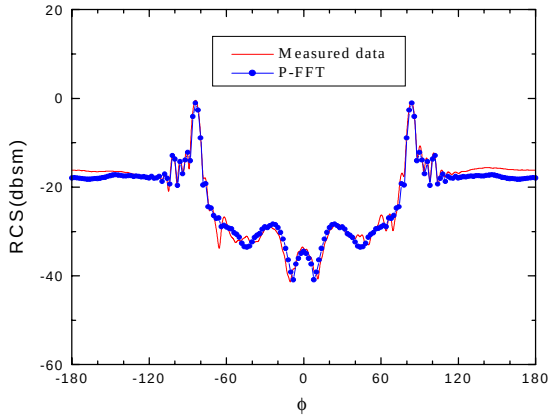

Figure 5. The monostatic RCS (θ polarization)

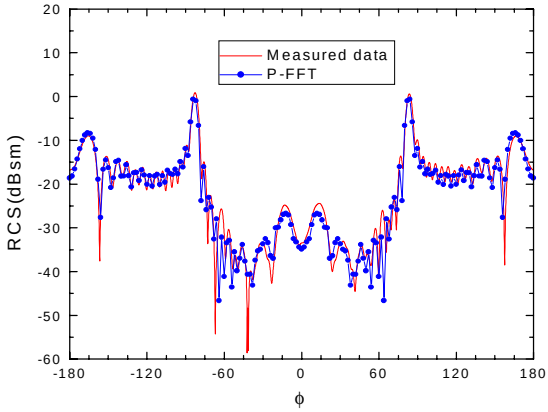

Figure 6. The monostatic RCS (φ polarization)

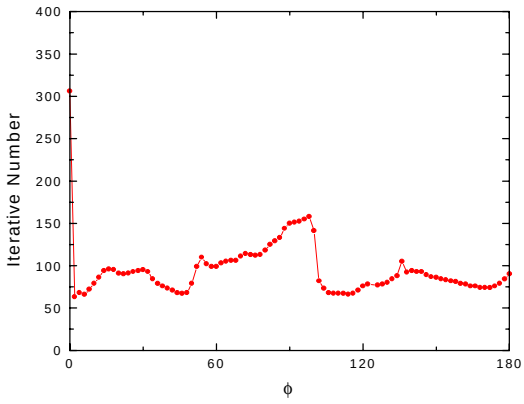

Figure 7. Number of iterations (θ polarization)

CONCLUSIONS

In this paper, the precorrected-FFT algorithm is successfully extended to the analysis of electromagnetic scattering problems in three dimensions. The generalized conjugate residual method (GCR) is used to solve the matrix equation derived from the discretization of the integral equation, then the precorrected-FFT technique is used to accelerate the matrix-vector multiplication in iterations. The memory requirement and computation complexity of the matrix-vector multiplication is reduced to $O(N_g)$ and $O(N_g \log N_g)$, respectively, where N_g denotes the number of the grid. Numerical examples demonstrated that the P-FFT yields a dramatic reduction of memory requirement and computational cost for large problems while remaining a good accuracy. Investigations also show that the P-FFT can have much coarser grid than AIM for the same error, thus leads to lower computational requirements than AIM. Besides, the P-FFT employs a multipole-based projection operator which is identical for every cell, so avoiding the complex and time consuming computations of the multipole moments of the basis functions for each cell as in the AIM. This also helps to save some computational costs.

Since the P-FFT is based on the fast Fourier transform and local interpolation operators, rather than on sphereical-harmonics based shifting operators as in the fast multipole method, a large range of kernels can be treated by this method while the high order of accuracy of fast multipole-based representations is still preserved. This implies that the algorithm can be readily further extended to more complicated problems with appropriate modifications.

REFERENCES

[1] R. Coifman, V. Rokhlin, and S. Wandzura, "The Fast Multipole Method for the Wave Equation: A pedestrian prescription", *IEEE Antennas Propagat. Mag*., vol.35, no. 3, pp. 7-12, June 1993.

[2] J. M. Song and W. C. Chew, "Fast Multipole Method Solution Using Parametric Geometry", *Microwave Opt. Technol. Lett.*, vol.7, no.16, 1994, pp.760-765.

[3] J. M. Song, C. C. Lu, W. C. Chew, "Multilevel Fast Multipole Algorithm for Electromagnetic Scattering by Large Complex Objects", *IEEE Trans. on Antennas and Propagation*, vol. AP-45, no. 10, pp. 1488-1493, Oct., 1997.

[4] E. Bleszynski, M. Bleszynski and T. Jaroszewicz, "A Fast Integral Equation Solver for Electromagnetic Scattering Problems", *IEEE APS Int. Symp. Dig.*, vol. 1, pp. 416-419, 1994.

[5] T. K. Sarkar, E. Arvas, and S.M. Rao, "Application of FFT and the Conjugate Gradient Method for the Solution of Electromagnetic Radiation from Electrically Large and Small Conducting Bodies", *IEEE Trans. on Antennas and Propagation*, vol. 34, no. 5, pp. 635-640, May, 1986.

[6] J. R. Phillips and J. K. White, "A Precorrected-FFT Method for Capacitance Extraction of complicated 3-D Structures", *Int. Conf. On Computer-Aided Design*, Santa Clara, California, Nov., 1994

[7] J. R. Phillips and J. K. White, "A Precorrected-FFT method for Electrostatic Analysis of Complicated 3-D Structures", *IEEE Trans. on Computer-Aided Design of Integrated Circuits and Systems*, vol.16, No.10, pp. 1059-1072, Oct., 1997.

[8] X. C. Nie, N. Yuan , L. W. Li and J. K. White, "Fast Solutions to Electromagnetic Scattering Problems Using Precorrected-FFT Method", submitted to *IEEE Trans. Antennas Propagat*

[9] S. M. Rao, D. R. Wilton and A. W. Glisson, Electromagnetic Scattering by Surfaces of Arbitrary Shape. *IEEE Trans. on Antennas and Propagation*, vol. 30, no.3, pp. 409-418, May,1982.

[10] Y. Saad and M. H. Schultz, "GMRES: A generalized minimal residual algorithm for solving nonsymmetric linear systems", *SIAM Journal of Sci. Statist. Comput.*, vol. 7, no. 3, pp. 856-869, July, 1986.

[11] E.O. Brigham, *The fast Fourier Transform and its applications.* Englewood Cliffs: Prentice-Hall, 1988

[12] A. D. McLaren, "Optimal Numerical Integration on a Sphere", *Mathematics of Computation*, vol. 17, pp. 361-383, 1963.

[13] S. S. Bindiganavale, J. L. Volakis, "Scattering From Planar Structures Containing Small Features Using the Adaptive Integral Method (AIM)", *IEEE Trans. on Antennas and Propagation*, vol.46, no.12, pp. 1867-1878, Dec., 1998.

[14] H. T. Anastassiu, M. Smelyanskiy, S. Bindiganavale, J. L. Volakis, " Scattering from relatively flat surfaces using the adaptive integral method", Radio Science, vol.33, no.1, pp. 7-16, Jan.-Feb., 1998.

[15] J. J. Bowman, T. B. A.Senior and P. L. E. Uslenghi, *Electromagnetic and Acoustic Scattering by Simple Shapes.* Hemisphere Publishing Corporation, New York, 1987, p.395

[16] A. C. Woo, H. T. G. Wang, M. J. Schuh, "Benchmark Radar Targets for the aalidation of Computational Electromagnetics Programs", *IEEE Antennas and Propagation Magzine*, vol. 35, pp. 84-89, 1993.